

# RADIATION FROM AN EXPANDING COCOON AS AN EXPLANATION OF THE STEEP DECAY OBSERVED IN GRB EARLY AFTERGLOW LIGHT CURVES

ASAF PE'ER<sup>1,2</sup>, PETER MÉSZÁROS<sup>2</sup> AND MARTIN J. REES<sup>3</sup>

*Draft version September 11, 2018*

## ABSTRACT

Observations of early afterglow emission from gamma-ray bursts (GRB's) with the *Swift* satellite show steep decay of the X-ray light curve,  $F_\nu(t) \propto t^{-\alpha}$  with  $\alpha \approx 2.5 - 4$  at  $\sim 300 - 500$  s after the burst trigger. The spectrum in this time interval is consistent with a spectrum  $F_\nu \propto \nu^{-\beta}$  with  $\beta \approx 1$ . Here, we show that these results can be explained as due to emission from the hot plasma “cocoon” associated with the jet, which expands relativistically after the jet has broken through the stellar envelope, if a substantial fraction of the cocoon kinetic energy is dissipated at scattering optical depths  $\tau_T \sim 10^2 - 10^3$ . This results in the bulk of the cocoon photons being observed at X-ray energies, after a delay of few hundreds of seconds relative to the gamma-ray photons from the jet. Multiple Compton scattering inside the cocoon causes a spread in the arrival times of the X-ray photons. We calculate numerically the observed light curve of photons emerging from the cocoon, and show that it exhibits a steep decay, which resembles that observed in many GRB afterglows. During the adiabatic expansion that follows the dissipation phase, photons lose energy to the expanding plasma, and as a result, the emerging photon energy distribution differs from a black-body spectrum, and can be approximated as a power law in the *Swift* XRT band. Comparison of the numerical results with the *Swift* XRT data of GRB050315 and GRB050421 shows good agreement between the light curves and spectra during the initial steep decay phase.

*Subject headings:* gamma rays: bursts — gamma rays: theory — plasmas — radiation mechanisms: non-thermal — radiative transfer

## 1. INTRODUCTION

The successful launch of the *Swift* gamma-ray bursts (GRB) explorer (e.g., Gehrels *et al.* 2004) enabled to probe X-ray afterglow emission at early times ( $\sim 10^2$  s to  $\sim 10^4$  s) after the burst onset, a time interval which was largely unexplored previously. The early afterglow observations revealed an unexpectedly steep decline in the X-ray light curves of  $\sim 2/3$  of the bursts that did not show flaring activity,  $F_\nu(t) \propto t^{-\alpha}$  with  $\alpha \approx 2.5 - 4$  following the prompt emission and lasting few tenths - hundreds of seconds. The steep decline in the light curve is followed by a much shallower decay,  $\alpha \approx 0.7$  at later times (Tagliaferri *et al.* 2005; Chincarini *et al.* 2005; Zhang *et al.* 2006; Nousek *et al.* 2005; O'Brien *et al.* 2006). The steep decay segment observed by the X-ray telescope (XRT; Burrows *et al.* 2005) usually connects to the spectral extrapolation of the Burst Alert Telescope (BAT; Barthelmy *et al.* 2005a) prompt emission light curve smoothly (Cusumano *et al.* 2006; Barthelmy *et al.* 2005b; Hill *et al.* 2006).

The spectral index obtained by the XRT in the 0.3-10 keV range during the steep decay segment of the light curve is close to unity,  $F_\nu \propto \nu^{-\beta}$ , with  $\beta \simeq 1$  (O'Brien *et al.* 2006). This power law index is somewhat softer than the power law index obtained at higher energies by the BAT data, at 15-150 keV.

A possible explanation to the steep decline observed in many light curves was suggested by Zhang *et al.*

(2006) and Nousek *et al.* (2005) (see also Liang *et al.* 2006). According to their suggestion, the steep decline is due to the effect known as “the curvature effect” (Fenimore *et al.* 1996; Kumar & Panaitescu 2000; Dermer 2004). In this effect, radiation arising from high angular latitude relative to the viewing direction arrives to the observer at late times, following the termination of the prompt emission, due to the extra distance it travels. In addition, this radiation is observed at flux and peak frequency lower than the corresponding in the prompt emission radiation, due to the beaming effect. This model predicts a connection between the temporal and spectral indices of the emission (Kumar & Panaitescu 2000; Dermer 2004; Zhang *et al.* 2006): in the relation  $f_\nu(t) \propto t^{-\alpha}\nu^{-\beta}$ ,  $\alpha$  and  $\beta$  are related via  $\alpha = 2 + \beta$ . However, a detailed analysis of 40 XRT light curves by O'Brien *et al.* (2006) found that the spectral and temporal indices are uncorrelated, in contrast to this model prediction. Moreover, when fitting the light curves in a model that allows stretching and shifting of the trigger time, O'Brien *et al.* (2006) found that 6 out of the 40 bursts show spectral decay index larger than the allowed value of the high latitude emission model prediction.

In recent years, there is increasing evidence that long duration ( $t_{90} \geq 2$  s; Kouveliotou *et al.* 1993) GRB's are associated with the deaths of massive stars, presumably arising from core collapse (Woosley 1993; Levinson & Eichler 1993; MacFadyen & Woosley 1999; MacFadyen *et al.* 2001; Zhang *et al.* 2003) (see also Pe'er & Wijers 2005, for short summary of observational evidence). In this so called “collapsar” model (Woosley 1993; Paczyński 1998), the collapse of the Fe core of a massive star leads to the formation of a central black hole (BH) of several solar masses. A rela-

<sup>1</sup> Astronomical Institute “Anton Pannekoek”, Kruislaan 403, 1098 SJ Amsterdam, the Netherlands; apeer@science.uva.nl

<sup>2</sup> Dpt. Astron. & Astrophysics, Dpt. Physics, Pennsylvania State University, University Park, PA 16802

<sup>3</sup> Institute of Astronomy, University of Cambridge, Madingley Rd., Cambridge CB3 0HA, UK

tivistic jet is thought to arise during this short accretion period (Aloy *et al.* 2000; MacFadyen *et al.* 2001). As the light (compared to the stellar density), relativistic jet makes its way out of the progenitor star, its rate of advance is slowed down, and most of the energy output during that period is deposited into a hot cocoon surrounding it (Mészáros & Rees 2001; Matzner 2003; Ramirez-Ruiz *et al.* 2002).

The jet head propagates through the Fe and He core of the star, until it emerges from the He core into the low density H envelope at  $r_* \approx 10^{11}$  cm (MacFadyen & Woosley 1999; Mészáros & Rees 2001; Matzner 2003; Waxman & Mészáros 2003). Following the jet emergence, the hot plasma composing the cocoon (shocked jet material which accumulates while the jet forces its way out, entrained with material swept from the star) swiftly escapes from the stellar cavity and accelerates in approximately the same way as the plasma composing the jet - its energy is converted via adiabatic expansion into bulk kinetic energy (Mészáros & Rees 2001; Ramirez-Ruiz *et al.* 2002). The entropy per baryon in the cocoon,  $\eta_c = (L_c/\dot{M}c^2)$ , is smaller than the entropy per baryon in the jet, due to the entrainment of the cocoon with material from the star. The cocoon therefore accelerates up to an asymptotic Lorentz factor which is lower than the Lorentz factor of the jet (but still, relativistic), before dissipating its kinetic energy.

The larger number of baryons in the cocoon compared to the jet baryon load implies that if the cocoon kinetic energy is dissipated at similar radii to the dissipation radius of the jet kinetic energy (e.g., by magnetic reconnection, as suggested by Thompson (1994) and Giannios & Spruit (2005), or alternatively by shock waves), than the optical depth for scattering of photons inside the cocoon at the dissipation radius is very large,  $\tau_{\gamma e} \sim 10^2 - 10^3$ . As a result, these photons cannot emerge from the cocoon immediately, and are diffused out during the adiabatic expansion that follows the dissipation. These photons thus suffer a significant time delay compared to photons that were emitted from the jet as the jet kinetic energy was dissipated, which produce the observed prompt emission. Moreover, the multiple scattering of these photons inside the cocoon produces a spread in the escape times of these photons, which - as we show below - can result in the steep slopes in the early afterglow light curves observed by the *Swift*.

In this paper, we analyze the emission from the expanding cocoon, and show that it can provide a natural explanation to the observed decline in the early afterglow light curves. We calculate in §2 the diffusion time delay of the cocoon photons. In §3 we present numerical results of the light curves and spectra. We show that the resulting spectra is much flatter than black-body spectrum, due to the multiple scattering by the cocoon plasma electrons, during the cooling down of the electrons in the adiabatic expansion that follows the dissipation. We compare our results with the *Swift* data in §4, before summarizing in §5.

## 2. SCALING LAWS FOR THE TIME DELAY AND TEMPERATURE OF COCOON PHOTONS

Following the emergence of the relativistic jet from the star (e.g. a WR star), the hot plasma composing the cocoon escapes from the jet cavity. As pointed out by

Lazzati & Begelman (2005), the jet opening angle at breakout is  $\lesssim 1^\circ$ , while the cocoon opening angle is of the order of tens of degrees. Following its emergence, the cocoon expands in all directions in the dilute stellar wind or dilute H-envelope (if any). At this stage, the lateral expansion velocity of the cocoon is close to the speed of light, and the cocoon expansion becomes isotropic (e.g., Aloy *et al.* 2000). We can therefore approximate the cocoon geometry in its expansion phase as spherical.

During the cocoon expansion, which lasts few - few tens of seconds (see below), the inner engine that produces the jet may still remain active. Therefore, during the cocoon expansion, fresh jet material continuously passes through the cocoon, in a similar way to jet propagation in the core of the star, thus keeping the cocoon channel open. During its expansion the cocoon pressure decreases, therefore the jet material passing through the cocoon is less tightly collimated, resulting in an increase of the jet opening angle as it passes through the cocoon (e.g., see discussion in Lazzati & Begelman 2005).

Dissipation of the jet kinetic energy produces the prompt  $\gamma$ -ray emission. This dissipation can be caused by e.g., internal collisions or magnetic reconnection occurring at radii larger than that of the leading edge of the cocoon (which is less relativistic than the jet,  $\Gamma_{co} \sim 10$  vs.  $\Gamma_{jet} \gtrsim 100$ ). Thus, the cocoon does not interfere with the usual jet prompt emission production. The presence of features in the early X-ray light curve such as X-ray bumps or flares, or a shallow X-ray decay phase, should also be compatible with the presence of a cocoon. While specific mechanisms for flares and shallow decays are not considered here, if these are produced, e.g. by late internal shocks or continued injection of energy into the jet, a requirement is that the funnel drilled by the jet inside the cocoon remains open during the prompt and early afterglow emission phase. This is plausible e.g. in a late internal shock or continued ejection model, where material continues to flow out in the jet. This in turn, suggests that disturbances and oblique shocks in the expanding cocoon, caused by the continued jet activity, can lead to additional dissipation throughout the cocoon volume, in addition to the cocoon interaction with the external medium or wind. Photons emitted in the jet, whether prompt  $\gamma$ -rays, early flares or shallow decay, are expected to escape immediately, provided as usual that they are emitted above the jet photosphere. They are also beamed into a solid angle smaller than the jet opening angle. However, photons emitted in the cocoon surrounding the jet cannot escape directly, due to the high optical depth in the cocoon.

The cocoon photons are therefore observed with a time delay compared to the prompt  $\gamma$ -ray photons emitted from the jet (although they can arrive before the photons produced by late internal shocks or refreshed shocks in the jet which might produce flares and shallow decays). This time delay relative to the prompt  $\gamma$ -rays has three different sources. First,  $\Delta t_g$  is the "geometrical" time delay, representing the time delay of photons originating from different regions in the flow compared to photons originating from the line of sight toward the observer. Second,  $\Delta t_{esc}$  is the time delay resulting from the finite time it takes the cocoon plasma to emerge from the Fe/He core of the star, following the emergence of the jet. Third,  $\Delta t_D$  is the diffusion time delay, which is the time

it takes the cocoon photons to escape from the cocoon plasma.

In order to estimate these time delays, we assume that both the cocoon and the jet emerge from the core of the star at  $r_* = 10^{11} r_{*,11}$  cm (Mészáros & Rees 2001; Waxman & Mészáros 2003; Matzner 2003; Lazzati & Begelman 2005). After the jet drills its way through the core of the star, it propagates through the H envelope, if any, and escapes, producing the “prompt”  $\gamma$ -ray emission at some usual nominal radius  $r_i \simeq 10^{13} r_{i,13}$  cm, where the jet is already optically thin. Relative to some nominal signal emitted from the base of the flow, these photons reach the observer subject to a geometrical time delay  $\Delta t_{g,jet} \simeq r_i / (4\Gamma_j^2 c) \simeq 8 r_{i,13} \Gamma_2^{-2}$  ms, due to the finite width and angular size of the jet emitting region.

The cocoon starts its acceleration once it emerges from the core of the star, when the jet has broken through. We approximate the time it takes the cocoon plasma to emerge from the core as  $\Delta t_{esc} = f r_* / c_s \simeq 6 r_{*,11} f_0$  s, where  $c_s = c / \sqrt{3}$  is the speed of sound and  $f \geq 1$  is an unknown numerical factor which accounts for the excess of time (above the free expansion time) it takes the cocoon to emerge from the core, and is taken here to be  $f = 1 f_0$ . To estimate the total energy in the cocoon, we start from the Frail et al (2001) value for the typical (collimation corrected) jet energy,  $E_j \sim 10^{51}$  erg, with a spread of about one order of magnitude. This refers mainly to the electron component, so conservatively one can multiply by a factor 3 for the proton energy in the jet. The cocoon is fed by the total output of the jet while the latter expands subrelativistically inside the star, and assuming a factor  $\sim 3$  longer jet lifetime inside the star than outside it, the cocoon total energy may be taken as  $E_c \sim 10^{52} E_{c,52}$  erg. The baryon mass in the cocoon is also expected to be significantly larger by an uncertain value than that in the jet, due to entrainment of baryons from the stellar envelope. The entropy per baryon in the cocoon plasma is likely to be lower than that of the jet, and is parametrized here as  $\eta_c = 10 \eta_{c,1}$ . Following its emergence from the core of the star, the cocoon expands spherically and accelerates up to a cocoon saturation radius,  $r_{s,c} = r_* \eta_c = 10^{12} r_{*,11} \Gamma_{c,1}$  cm, where  $\Gamma_c = \eta_c = 10 \Gamma_{c,1}$  is the asymptotic value of the cocoon Lorentz factor (e.g., Ramirez-Ruiz et al. 2002). Assuming isotropic expansion of the cocoon outside the core, the comoving cocoon width is estimated by  $\Delta r_c \simeq \Gamma_c r_* = 10^{12} r_{*,11} \Gamma_{c,1}$  cm.

The cocoon energy release can be approximated as an impulsive release involving a single pulse of width  $\Delta t_{esc}$ . Thus, at a radius  $r_{i,c} > r_{s,c}$  where dissipation of the cocoon kinetic energy occurs (e.g. via internal shocks, reconnection, etc), the cocoon comoving proton density can be estimated as  $n_p(c) = E_c / (4\pi r_{i,c}^3 m_p c^2)$ , where  $E_c$  is the energy content of the cocoon. For dissipation at a radius  $r_{i,c}$  below the cocoon photospheric radius where the cocoon becomes optically thin, the cocoon optical depth to scattering is given by

$$\tau_{\gamma e,c} = \Delta r_c n_p(c) \sigma_T \simeq 350 E_{c,52} r_{*,11} r_{i,13}^{-3} \Gamma_{c,1}, \quad (1)$$

where  $E_c = 10^{52} E_{c,52}$  erg. Thus, for dissipation radii anywhere between the stellar radius  $r_{*,11}$  and the cocoon photosphere at  $r \sim 10^{14}$  cm, the optical depth to

scattering inside the cocoon is high. Therefore, photons that are produced inside the cocoon suffer, in addition to a geometrical time delay as they emerge from the photosphere,  $\Delta t_{g,c} = r_{ph} / 4\Gamma_c^2 c$ , also a diffusive time delay before they escape.

The diffusive time delay is estimated as follows. Following the dissipation phase, the cocoon expands in its rest frame at the speed of sound. The electron temperature inside the cocoon is mildly relativistic,  $kT' / m_e c^2 \simeq 10^{-3}$  (see below), and the cocoon is radiatively dominated, therefore the cocoon expansion speed is close to the asymptotic value  $v \lesssim c / \sqrt{3}$ . The rapid expansion implies that the mean free path of photons inside the cocoon increases with (comoving) time as  $l(t) \simeq l_0 (vt / \Delta r_c)^3$ , where  $l_0 = \Delta r_c / \tau_{\gamma e,c}$  is the mean free path at the end of the dissipation phase, and a constant expansion velocity  $v$  assumed. For a large number of scatterings,  $\tau_{\gamma e,c} \gg 1$ , the distance traveled by a photon before it escapes is  $ct = \int (dl(t) / dt) dt$ , where  $t$  is the comoving time from photon production to escape. We thus find that the comoving diffusion time is

$$t \equiv \Delta t_D^{co} \simeq \frac{\sqrt{\tau_{\gamma e,c}} \Delta r_c}{c}, \quad (2)$$

and the observed diffusive time is shorter by a factor of  $\Gamma$ . A full analytical treatment presented in §A gives a numerical pre-factor  $3^{3/4}$  (for  $v = c_s$ ). An alternative calculation of the time delay can be carried out using the fact that the photons emerge from the expanding plasma as they reach the photospheric radius,  $r_{ph}$ . We show in §B that the two approaches yield similar results. Nonetheless, the advantage of the calculation as presented here is that it can be generalized to the calculation of the spread in the photon arrival time, which results in the steep decay (see §3 below).

The comoving temperature of the cocoon plasma at the dissipation radius is calculated as follows. During the cocoon emergence time from the star  $\Delta t_{esc}$ , the cocoon expands to a radius  $\sim \Delta t_{esc} \times c_s$ , thus the cocoon occupies a volume  $V_c = (4\pi/3)(f r_*)^3$ . As it emerges from the core of the star, the cocoon temperature  $T'(r_c)$  is calculated using  $E_c / V_c \simeq a T'(r_c)^4$ , where  $a$  is Stefan’s constant. At  $r < r_{s,c}$ ,  $T'(r) \propto r^{-1}$ , and at larger radii.  $T'(r) \propto r^{-2/3}$ . We thus find that at the dissipation radius,

$$T'(r_i) = \left( \frac{3E_c}{4\pi(f r_*)^3 a} \right)^{1/4} \left( \frac{r_{s,c}}{r_*} \right)^{-1} \left( \frac{r_i}{r_{s,c}} \right)^{-2/3}. \quad (3)$$

The normalized cocoon temperature at the dissipation radius is therefore equal to

$$\theta_{el} \equiv \frac{k_B T'}{m_e c^2} = 5 \times 10^{-4} E_{c,52}^{1/4} r_{*,11}^{-1/12} r_{i,13}^{-2/3} \Gamma_{c,1}^{-1/3} f_0^{-3/4}. \quad (4)$$

### 3. LIGHT CURVE AND SPECTRA OF PHOTONS EMERGING FROM THE COCOON

While the details of the dissipation process are uncertain, the high optical depth inside the cocoon implies that photons undergo multiple Compton scattering before they escape, hence the resulting spectrum is expected to be quasi-thermal irrespective of the details of the dissipation process. Following the dissipation, the

plasma expands and cools. During the cooling phase, the plasma electrons are coupled to the photons via Compton scattering. The total energy in the photon component cannot exceed the total energy dissipated by the electrons at the dissipation phase, which is approximated by a fraction  $\epsilon_e \leq 0.33$  of the total dissipated energy. As shown by Pe'er & Waxman (2004), photons are expected to give up to  $\sim 2/3$  of their energy to the plasma during the expansion phase that follows the dissipation. The plasma energy therefore increases by a factor smaller than  $\sim 20\%$  of its initial energy during the expansion phase.

In addition to Compton scattering, possible sources of electrons energy loss during the expansion phase are synchrotron radiation and bremsstrahlung emission. Synchrotron losses depend on the uncertain value of the magnetic field. An upper limit on this value during the dissipation phase can be found by assuming equipartition (a fraction  $\epsilon_B \approx 0.33$  of the cocoon internal energy density is converted to magnetic field), which results in a value  $B \simeq 10^6 B_6$  G. The characteristic momentum of electrons having Maxwellian distribution with temperature  $\theta_{el} \ll 1$  is  $\gamma\beta \simeq \theta_{el}^{1/2}$ . The cyclo-synchrotron power radiated by these electrons is therefore  $P_{syn,0} = (4/9)[q^4 B^2 (\gamma\beta)^2] / (m_e^2 c^3) \simeq 10^{-6} B_6^2 \theta_{el,-3} \text{ erg s}^{-1}$ , where  $\theta_{el} = 10^{-3} \theta_{el,-3}$  is used (see eq. 4). The magnetic field, though, decreases quickly during the expansion phase. Denoting by  $R(t)$  the characteristic cocoon radius at time  $t$ , the number and energy density of electrons decrease as  $n_{el}(t), u_{el}(t) \propto R(t)^{-3}$ , thus  $B(t) \propto R(t)^{-3/2}$  at times  $t > t_0$ , where  $t_0$  marks the beginning of the expansion phase. For  $t \gg t_0$ ,  $R(t) \simeq c_s(t - t_0)$  where  $c_s$  is the speed of sound (see below), therefore  $P_{syn}(t) \propto t^{-3}$ . We thus conclude, that shortly after the beginning of the expansion, at  $t \gtrsim (\Delta r_c / c_s)(P_{syn,0} t_{dyn} / m_e c^2)^{1/3}$  the electron energy loss time becomes longer than the dynamical time, which is comparable to the comoving diffusion time  $t_{dyn} \simeq \Delta t_D^{co}$ . As a result, synchrotron losses do not affect the dynamics of the plasma during the expansion phase.

A similar conclusion can be drawn for bremsstrahlung emission. The rate of energy loss of electron by bremsstrahlung radiation during the dissipation is given by (see, e.g., Rybicki & Lightman 1979)  $P_{brem} = (2\pi^3 \theta_{el} / 3)^{1/2} (2^5 q^6 / 3 h m_e c^2) n_{el} \bar{g}_B \simeq 1.3 \times 10^{-9} \theta_{el,-3}^{1/2} n_{el,14.5} \text{ erg s}^{-1}$ , where  $n_{el} = n_p(c) = 10^{14.5} n_{el,14.5} \text{ cm}^{-3}$  is the electrons number density at the dissipation, and  $\bar{g}_B$  is the averaged Gaunt factor. Since the electrons number density decreases quickly with time, we conclude that bremsstrahlung losses are insignificant. We can therefore approximate the expansion as adiabatic.

During the expansion phase, the expansion velocity of a plasma element (in its comoving frame) depends on the radial position of the element. The surface of the plasma expands at the velocity of sound, while internal parts expand at lower velocity,  $v(r) \propto r$ . The coupling of the expansion velocity to the position of a plasma element significantly complicates the problem<sup>4</sup>. In order

to calculate the emergence light curve and spectra, we therefore use a numerical code, based on Monte-Carlo method<sup>5</sup>.

### 3.1. The numerical model

We consider a three-dimensional uniform, homogeneous plasma ball that expands in its rest frame at radial velocity  $v(r) = [r/R(t)]c_s$ , where  $c_s = c/\sqrt{3}$  is the speed of sound, and  $R(t) = R_0 + c_s t$  is the ball radius at comoving time  $t$  after the dissipation (for convenience, we assume that the dissipation phase ends, and the adiabatic expansion begins at  $t = 0$ . Thus,  $R_0$  is the comoving plasma width at the end of the dissipation phase). The plasma is characterized by an initial optical depth to scattering  $\tau_{\gamma_e}(t = 0) = \tau_0$ . As a result of the expansion, the number density of particles inside the plasma decreases as  $n_{el} \propto R(t)^{-3}$ , and the optical depth decreases as  $\tau_{\gamma_e}(t) \propto R(t)n_{el}(t) \propto R(t)^{-2}$ . The particle inside the plasma assume a Maxwellian distribution with initial temperature given by equation 4. As discussed above, particle cooling during the expansion is insignificant compared to adiabatic cooling. Therefore, at  $t > 0$ , the particles cool adiabatically, hence their temperature decreases as  $\theta_{el}(t) \propto R(t)^{-2}$ .

Since during the dissipation phase energy is dissipated inside the entire comoving width of the cocoon, we assume here that photons are injected uniformly inside the ball at  $t = 0$ . We consider two types of energy distributions of the injected photons: (a) monoenergetic injection, with initial (comoving) energy  $\epsilon_0 = (k_B T'(r_i) / m_e c^2)$ , where  $T'(r_i)$  is the electrons temperature at the dissipation radius, given by equation 3; and (b) power law spectrum of the injected photons above  $\epsilon_0$ , with a power law index  $dn_\gamma/d\epsilon \propto \epsilon^{-2}$ .

The characteristic energy of synchrotron photons emitted during the expansion phase is at least seven orders of magnitude lower than the plasma energy ( $\epsilon_{syn} \lesssim 10^{-5}$  eV for  $B \sim 10^6$  G), therefore these photons are neglected. Similarly, the power radiated in bremsstrahlung emission during the expansion is at least three orders of magnitude lower than the emitted power during the dissipation phase. We therefore neglect in the numerical calculations additional sources of radiation during the expansion phase, and consider Compton (and inverse Compton) scattering only during this phase.

Photons interact with electrons inside the plasma ball via Compton scattering (no absorption is considered). In the calculation, the exact differential Compton cross section is used. For each escaping photon, the code traces its energy and the delay of the photon escape time compared to a hypothetical photon that was injected at the plasma center at  $t = 0$  and did not suffer any scattering before escaping the plasma.

### 3.2. Numerical results

The light curves obtained for three different values of the optical depth,  $\tau_{\gamma_e} = 10^1, 10^2, 10^3$ , and comoving

tons. This method, however cannot be implemented here because of the coupling between the comoving plasma radial velocity and the radius of the plasma,  $v(r) \propto r$ .

<sup>5</sup> We use a version of the Monte-Carlo code used in Pe'er & Waxman (2004) for the calculation of photons energy loss during the adiabatic expansion.

<sup>4</sup> Sunyaev & Titarchuk (1980) calculated analytically the light curve of photons escaping from a steady (non-expanding) plasma in the limit  $\tau_{\gamma_e} \gg 1$ , by solving the diffusion equation for pho-

width  $R_0 = 10^{12}$  cm in all three cases are presented in Figure 1. The cocoon isotropic equivalent dissipated energy is  $E_{c,52} = 0.3, 1, 3$  respectively, and we assume a redshift  $z = 1$  in a flat universe for calculating the observed flux. These values correspond to a kinetic energy dissipation phase that occurs at radii  $\approx 10^{13}$  cm (see eq. 1). The mean time delays of photons in the three presented graphs are 8, 60, 210 s for  $\tau_{\gamma e} = 10^1, 10^2, 10^3$  respectively. These values are in very good agreement with the analytical estimate of equation A2. Clearly, the light curves at late times decrease according to  $F_\nu(t) \propto t^{-\alpha}$  with  $\alpha \approx 3 - 4$ , irrespective of the exact value of the optical depth. Similar steep decrease in the light curves at late times was found by Sunyaev & Titarchuk (1980) for the case of non-expanding plasma and various geometries considered there. This suggests that a steep decrease in the light curve is a general property of emission from plasma characterized by number of scattering higher than few tens (in an expanding plasma, the mean number of scattering of a photon before it escapes is  $n_{sc.} \propto \tau_{\gamma e}$ , while in a steady plasma  $n_{sc.} \propto \tau_{\gamma e}^2$ ; see, e.g. Pe'er & Waxman 2004).

The emerging photons' spectra are presented in Figure 2. The photon injection is approximated as monoenergetic, with energy equal to the peak energy of the thermal distribution of the electrons,  $\varepsilon_0 = \theta_{el} m_e c^2 = 500$  eV (in the plasma frame). The observed energy of the injected photons is therefore  $\varepsilon_0^{ob.} = \varepsilon_0 \times \Gamma_c / (1 + z) = 2.5$  keV, where  $\Gamma_c = 10$  and redshift  $z = 1$  assumed. For high value of the optical depth, most of the photons lose energy before they escape. As shown in Pe'er & Waxman (2004), for  $\tau_{\gamma e} = 100$  about 70% of the energy lost by the photons is transferred to the bulk motion of the expanding plasma, and the remaining is transferred to thermal energy of the electrons. This energy loss results in the quasi-thermal spectrum obtained at low energies. Still, for a uniform injection of photons as is considered here, the high energy tail of the emerging photon spectra is a power-law like with power law index  $\beta \simeq 1$  ( $F_\nu \propto \nu^{-\beta}$ ), in the energy range 0.3–10 keV, which is the *Swift* XRT energy band. The case  $\tau_{\gamma e} = 1000$  presented in figure 2, shows an upper limit on the cocoon optical depth that is still consistent with the observations. Due to the large number of scattering, the photon index in the *Swift* XRT range is not well defined, and the data is marginally consistent with a power law index  $\beta \simeq 1$  in this range.

A similar result is obtained when one considers the more realistic case of power law photon injection above the characteristic energy  $\varepsilon_0^{ob.}$ , as is expected, e.g., if the main radiative mechanism is synchrotron radiation, or alternatively, multiple Compton scattering of a photospheric component (Pe'er *et al.* 2005). In figure 2, the dash-dotted line presents the case of power law injection of photons above  $\varepsilon_0^{ob.}$ , with power law index  $p = 2$ . In this case as well, the obtained spectral slopes have power law index  $\beta \simeq 1$  in the *Swift* XRT energy band.

#### 4. COMPARISON WITH DATA: THE CASES OF GRB050315 AND GRB050421

The steep decline in the XRT light curves observed in many bursts (O'Brien *et al.* 2006) is similar to the steep decline in the light curves obtained by the Monte Carlo simulation. We show in Figures 3,4 two fits of the data of

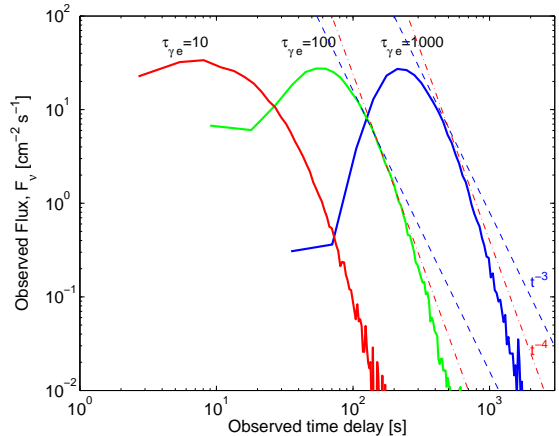


FIG. 1.— Light curves of photons emerging from an expanding cocoon, characterized by initial optical depths  $\tau_{\gamma e,c} = 10, 100, 1000$ . Initial comoving radius  $R_0 = 10^{12}$  cm, comoving temperature  $\theta_{el} = 10^{-3}$  injected photon energy  $\varepsilon_0 = 10^{-3}$  (in units of  $m_e c^2$ ), characteristic Lorentz factor  $\Gamma_c = 10$  and redshift  $z = 1$  are assumed. The dissipated cocoon isotropic equivalent energy  $E_{c,52} = 0.3, 1, 3$  respectively is considered. Photons are injected uniformly inside the sphere. Similar light curves are obtained for photon injection with power law energy distribution above  $\varepsilon_0$ . Each of the presented curves is produced by  $10^5$  Monte-Carlo runs.

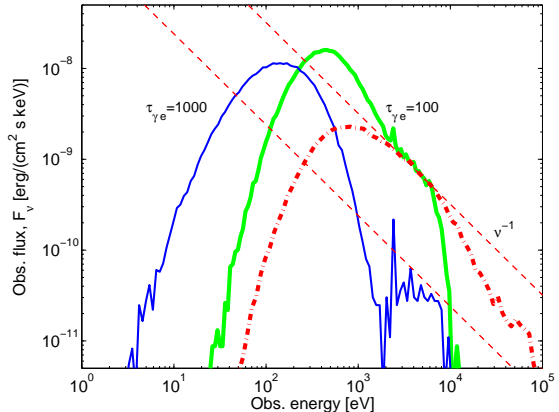


FIG. 2.— Resulting spectra of the emerging photons for the cases of  $\tau_{\gamma e,c} = 100, 1000$ . Solid lines present injection of monoenergetic photons at energy  $\varepsilon_0 = 10^{-3}$  (in units of  $m_e c^2$ ), and dash-dotted line presents injection of photons having power law energy distribution with power law index  $p = 2$  above  $\varepsilon_0$ , as might be expected from synchrotron emission above the peak and cooling frequencies. Thick lines are for  $\tau_{\gamma e} = 100$ , and the thin line presents the case of  $\tau_{\gamma e} = 1000$ . All other parameters are the same as in figure 1. For  $\tau_{\gamma e} = 100$ , the spectral slope in the XRT range (0.3 – 10 keV) is close to  $\beta = 1$ , while for  $\tau_{\gamma e} = 1000$  a single spectral slope is marginally consistent with this result.

GRB050315 and GRB050421 obtained from P. O'Brien by the numerical model results. These two bursts did not show significant flaring activity, and had a good time coverage during the steep decay phase of the emission.

In fitting the data we assumed a cocoon optical depth at the dissipation radius  $\tau_{\gamma e,c} = 100$ . This value is consistent with the assumption that the dissipation radius is  $\gtrsim 10^{13}$  cm. The redshift of GRB050315 is  $z = 1.949$  (Vaughan *et al.* 2006), and the redshift of GRB050421 is unknown, thus is taken here to be  $z = 1$ . The values of the cocoon Lorentz factors during the cocoon dissipation phase  $\Gamma_c$  were determined using the observed

time delays at the beginning of the decay. The resulting Lorentz factors,  $\Gamma_c = 30, 8$  in the two cases are of the same order of magnitude,  $\Gamma_c \sim 10$ . The value of the dissipated cocoon energy required to fit the data depends on the assumption about the injected photon distribution. In the case of GRB050315, an isotropic equivalent cocoon energy  $E_{c,52} = 1.5$  ( $E_{c,52} = 2.5$ ) is required in the monoenergetic (power law injection) scenario, while in the case of GRB050421 cocoon energy  $E_{c,52} = 0.03$  ( $E_{c,52} = 0.1$ ) is required in these two scenarios. The values found are consistent with the order-of-magnitude estimates presented in §2 based on theoretical arguments.

The data of GRB050421 (figure 4) shows clear distinction between the early shallow decay observed at the first  $\sim 30$  s, which is attributed to prompt emission, and the rise of the flux followed by a steep fall at  $\sim 100$  s which is attributed in our model to emission from the cocoon. This time separation is less significant in the case of GRB050315 presented in figure 3, where a flare at  $\sim 25$  s precedes the cocoon emission, which peaks at  $\sim 30$  s. We further discuss this time separation issue in §5 below.

Fitting of the XRT spectra in these two cases are presented in Figures 5, 6. In the cases presented, we use the same parameters of the fits presented in figures 3,4 with a re-normalization of the flux to the cocoon emission time. We assume initial normalized electrons temperature  $\theta_{el} = 10^{-3}$  and injected photon energy  $\varepsilon_0 = \theta_{el} m_e c^2 = 500$  eV in the monoenergetic injection case. In the power law photon injection assumption, a power law index  $p = 2$  above  $\varepsilon_0$  in the photon energy distribution is assumed.

In fitting the data of GRB050315, the numerical results were shifted by a factor of 1.2 (3) in the monoenergetic (power law) injection cases. A physical origin of these shifts is that the temperature of the cocoon is different than the assumed numerical value of  $\theta_{el} = 10^{-3}$  by equivalent factors. We can thus summarize that the comoving temperature of the cocoon is  $\theta_{el} = 8.3 \times 10^{-4}$  ( $3.3 \times 10^{-4}$ ) for the monoenergetic (power law) injections assumptions used. Similarly, the comoving temperature of the plasma for the case of GRB050421 is  $\theta_{el} = 10^{-2}$  ( $5 \times 10^{-3}$ ) for monoenergetic (power law) photon injection cases.

For GRB050315, the spectra of the BAT data at late times is fitted with the XRT data with a single power law (Vaughan *et al.* 2006). This is consistent with the numerical results of the light curve presented in Figure 5 for the more realistic scenario of power law injection of photons. BAT data of GRB050421 exists only at the first  $\sim 100$  s, before the steep decay phase of the light curve. We thus conclude that the BAT photons originate from the jet, and not from the cocoon plasma.

The two fits presented here are only representative cases. Similar fits can be obtained for many light curves in O’Brien *et al.* (2006) sample, which show power law indices during the decay phase in the range  $\alpha \simeq 2 - 4$ . The similarities found between the numerical model light curves for different values of the optical depth imply that the data can be fitted with various values of the free parameters  $\tau_{\gamma e, c}$  and  $\Gamma_c$ . However, the demand that  $\Gamma_c$  is of the order of few tens, and not larger than  $\sim 100$ , and the demand that the spectrum differs from a black-body restricts the optical depth in both cases considered here

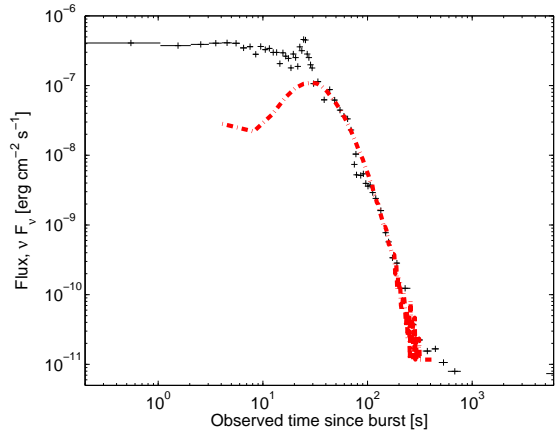


FIG. 3.— Fitting of the decline part in the XRT data of GRB050315 with the results of the numerical simulation light curve. Parameters used in the fitting are  $\tau_{\gamma e, c} = 100$ ,  $R_0 = 10^{12}$  cm,  $\Gamma_c = 30$ ,  $E_{c,52} = 2.5$  and  $z = 1.949$ .

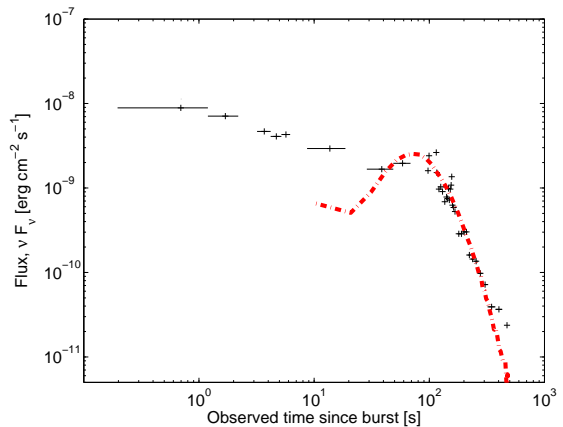


FIG. 4.— Fitting of the decline part in the XRT data of GRB050421 with the results of the numerical simulation light curve. Here,  $\Gamma_c = 8$ ,  $E_{c,52} = 0.1$  and  $z = 1$  were considered, and all other numerical free parameters have the same values as in figure 3.

to be  $\tau_{\gamma e, c} \sim 100$ .

The results presented here thus show that using values of the optical depth and cocoon temperature close to the “canonical” values considered in §2 (see eqs. 1, 4), emission from the cocoon can account for the observed steep decay spectra. The injected photons are assumed in all cases to have monoenergetic distribution at energy similar to the peak energy of the thermal electrons inside the cocoon, or to have a power law distribution above this energy. These photons therefore originate by dissipation mechanism inside the cocoon, without any assumptions on photons produced by the prompt emission. For assumed cocoon optical depth, by fitting the model to the data one can determine the values of the cocoon Lorentz factor  $\Gamma_c$ , the electrons temperature  $\theta_{el}$  and the dissipated cocoon energy,  $E_c$ .

## 5. SUMMARY AND DISCUSSION

In this paper, we have considered emission from an expanding cocoon as a possible explanation to the steep decay in the *Swift* XRT light curve observed in many bursts after few tens - few hundreds of seconds. We showed in §2

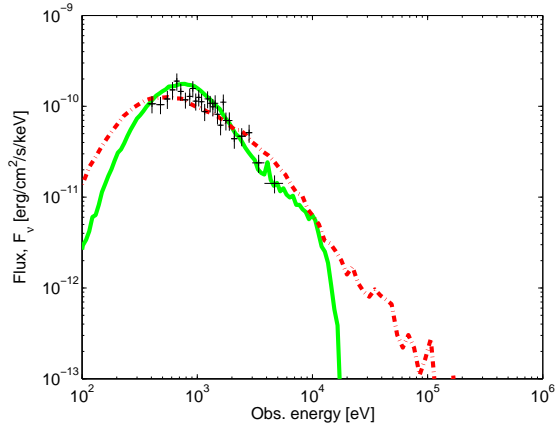


FIG. 5.— Fitting of the XRT spectrum of GRB050315 with the results of the numerical simulation light curves. Parameters used in the fitting are  $\tau_{\gamma e,c} = 100$ ,  $R_0 = 10^{12}$  cm,  $\Gamma_c = 30$  and  $z = 1.949$ . The cocoon energy and comoving temperature are  $E_{c,52} = 1.5$ ,  $\theta_{el} = 8.3 \times 10^{-4}$  for the mono-energetic (solid line),  $E_{c,52} = 2.5$ ,  $\theta_{el} = 3.3 \times 10^{-4}$  for the power law (dash dotted line) photon injection assumptions.

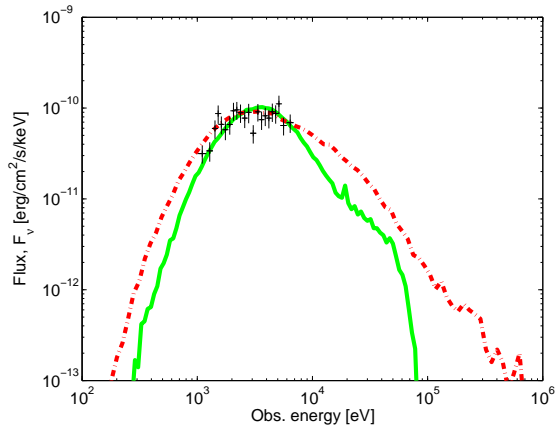


FIG. 6.— Fitting of the XRT spectrum of GRB050421 with the results of the numerical simulation light curves. Parameters used in the fitting are  $\tau_{\gamma e,c} = 100$ ,  $R_0 = 10^{12}$  cm,  $\Gamma_c = 8$  and  $z = 1$ . The cocoon energy and comoving temperature are  $E_{c,52} = 0.03$ ,  $\theta_{el} = 10^{-2}$  for the mono-energetic (solid line),  $E_{c,52} = 0.1$ ,  $\theta_{el} = 5 \times 10^{-3}$  for the power law (dash dotted line) photon injection assumptions.

that due to the high optical depth in the cocoon, photons produced inside the cocoon at similar radii to the estimated dissipation radius of the kinetic energy of the jet, are observed after a diffusion time delay of few hundreds of seconds. We then presented in §3 our numerical code, and showed the emergent photons light curve and spectra. We showed that the emergent photons light curves and spectra are similar to the decaying part of the light curves and the XRT spectra observed in GRB050315 and GRB050421, and argued that due to the similarities in many of the *Swift* XRT light curves, the numerical results fit the data in many bursts.

Due to the complexity of the problem, we did not obtain a simple analytical formulae for the light curves. However, we showed that the numerical results can be approximated as a power law over a limited time interval and energy range, which is similar to the energy range observed by the *Swift* XRT. Due to the large number of

scattering the photons undergo before they escape, the resulting spectrum in the XRT band is by large independent on the initial photons spectrum, which by itself depends on the details of the dissipation process. We therefore conclude that observations of the spectrum during the decay phase are not expected to unveil much of the mystery of the dissipation mechanism, if the cocoon model is correct.

We found that the shape of the light curves are similar for different values of the optical depth (figure 1). Light curves similar to the light curves presented here were also obtained by Sunyaev & Titarchuk (1980), for the case of non-expanding plasma. These facts suggest that the shape of the light curve may be common to many astrophysical phenomena in which photons undergo tens to hundreds of scattering before they escape the plasma in which they are produced. This may also explain the similarities found in the shape of the light curves in many different bursts in the sample of O’Brien *et al.* (2006).

These similarities also imply that the data could be fitted with various values of the free parameters -  $\tau_{\gamma e,c}$ ,  $\Gamma_c$  and the comoving temperature  $\theta_{el}$ . We showed in §4 two fits for the light curves and energy spectra of two different bursts, assuming that photons are produced at the dissipation inside the cocoon, without additional prompt emission photon source. We found that the fitted values of the cocoon Lorentz factor  $\Gamma_c$ , the cocoon energy  $E_c$  and the electrons temperature  $\theta_{el}$  are close to their “canonical” values calculated in §2 based on theoretical arguments. Restrictions on the values of these parameters are obtained from the physical demands that  $\Gamma_c$  is of the order of few tens, and not larger than  $\sim 100$ , and that the plasma temperature should not exceed the theoretical values predicted in §2.

The sample of Swift-XRT light curves presented in Figure 3 of O’Brien *et al.* (2006) shows significant variety. In many cases (e.g., GRB050319, GRB050412, GRB050422, GRB050713A, GRB050803 and many more), there is a clear distinction between the early (prompt) emission phase, and the steep decay phase. Following an early shallow decline, the flux rises before entering the steep decay phase. This pattern can be attributed to emission from the cocoon (see figure 1). In other cases (e.g., GRB050713B, GRB050814 and GRB 050819) a steep fall in the flux follows the end of the prompt emission, without a significant rise preceding the decay. In other cases, a shallow decay of the flux is observed over hundreds - thousands of seconds.

The model presented here suggests that (at least part of) these observations are the result of emission from the cocoon. The extension of the prompt emission to tens - hundreds of seconds implies that in many cases the emission from the cocoon is partially obscured by the prompt emission. This may explain the lack of rise in the flux in many cases which show steep decay. Obviously, the model presented here cannot account for the entire variety of the light curves observed. Nonetheless, the facts that rise in the flux was observed prior to the steep decay in several cases, and the steepness of the decay -  $\alpha \approx 2.5 - 4$  in many cases, are difficult to account for in models that do not consider the existence of the cocoon.

In addition to the many cases of long bursts which show a steep decline in the XRT light curve, a similar behavior was observed in one case of a short burst - GRB050724.

While the nature of short bursts progenitors is still not fully understood, it is most likely that these bursts do not originate from the explosion of massive stars, hence the cocoon model cannot be similarly motivated in this case. The decay observed in GRB050724 is so far unique, and was not observed in other short bursts. The present explanation, which applies to long bursts, does not preclude a high-latitude emission effect interpretation in some bursts, e.g., in short bursts, or in some fraction of long bursts.

Our model assumes an unspecified dissipation mechanism that converts cocoon kinetic energy into radiation at radii  $\lesssim 10^{13}$  cm, below the radius where the cocoon becomes optically thin to scattering. This radius could be as low as the stellar surface  $r \sim 10^{11}$  cm, but could be anywhere up to the photosphere. Such a dissipation may be caused by magnetic reconnection (Giannios & Spruit 2005), interaction with the expanding envelope of the star (Mészáros & Rees 2001) or extended central engine activity and refreshed shocks in the jet that could interact laterally with the cocoon region, and may derive oblique shocks into the cocoon. As presented in §B, similar time delays would in principle occur if the cocoon photons were advected from the core of the star, without any dissipation of the cocoon kinetic energy at larger radii. However, in this latter case the very high optical

depth at  $\sim 10^{11}$  cm would imply that the emergent spectrum is very close to black-body, which for the bursts discussed here is not consistent with the observations.

In contrast to the internal collision model, which predicts multiple dissipation phases resulting in long duration prompt emission, the cocoon model predicts only a single dissipation phase of the cocoon plasma. This model therefore disfavors a second phase of steep decay. The flares that are observed in many bursts thus are predicted to have a different source, e.g., extended central engine activity. Nonetheless, as discussed above, if the dissipation of the jet kinetic energy occurs at small enough radii where the optical depth is higher than a few tens, similar light curves are expected.

We wish to thank Paul O'Brien and Dave N. Burrows for useful discussions, and Paul O'Brien and Kim Page for providing us the data of GRB050315 and GRB050421. AP wishes to thank Ralph A.M.J. Wijers and Ed van den Heuvel for useful discussions. This research was supported by NWO grant 639.043.302, by the EU under RTN grant HPRN-CT-2002-00294 and by NSF AST0307376, NASA NAG5-13286 and NSF PHY99-07949.

## APPENDIX

### THE DIFFUSIVE TIME DELAY IN AN EXPANDING PLASMA

Assuming that following the dissipation phase the cocoon plasma expands at velocity close to its asymptotic velocity,  $c_s = c/\sqrt{3}$  the mean free path of photons increases with comoving time as  $l(t) = l_0(1 + vt/\Delta r)^3$ , where  $l_0 = \Delta r_c/\tau_{\gamma e,c}$  is the mean free path at the end of the dissipation phase, and constant expansion velocity  $v = c_s$  assumed. For a large number of scattering,  $\tau_{\gamma e,c} \gg 1$ , the distance traveled by a photon before it escapes is

$$c\Delta t_d^{co.} = \int_0^{\Delta t_d^{co.}} \frac{dl}{dt} dt = l_0 \left( 1 + \frac{v\Delta t_d^{co.}}{\Delta r_c} \right)^3 \approx \frac{\Delta r_c}{\tau_{\gamma e,c}} \left( \frac{v\Delta t_d^{co.}}{\Delta r_c} \right)^3, \quad (A1)$$

where  $\Delta t_d^{co.}$  is the comoving photon diffusion time. We thus find that in the observed frame, the diffusion time is given by

$$\begin{aligned} \Delta t_d &= \frac{\Delta t_d^{co.}}{\Gamma_c} \approx \sqrt{\frac{c}{v^3}} \frac{\sqrt{\tau_{\gamma e,c}} \Delta r_c}{\Gamma_c} \simeq 3^{3/4} \frac{\sqrt{\tau_{\gamma e,c}} \Delta r_c}{c\Gamma_c} \\ &= 250 E_{c,52.5}^{1/2} \tau_{*,11}^{3/2} r_{i,13}^{-3/2} \Gamma_{c,1}^{1/2}. \end{aligned} \quad (A2)$$

The diffusive time delay calculated above is of the order of few hundreds of seconds for the assumed values of the free parameters. This time delay is much longer than the escape time delay of the cocoon plasma from the core of the star  $\Delta t_{esc}$ , and it is longer than the geometrical time delay  $\Delta t_{g,jet}$  of the prompt radiation from the jet, but it is comparable to the geometrical time delay from the photosphere of the cocoon,  $\Delta t_{g,c}$ , as long as the optical depth to scattering inside the cocoon is high.

### ALTERNATIVE APPROACHES FOR THE CALCULATION OF THE DIFFUSION TIME DELAY

Photons that are produced in an expanding plasma in regions of high optical depth (i.e., at dissipation radii  $r_D \ll r_{ph}$ ) emerge from it as the plasma reaches the photospheric radius,  $r_{ph}$ . The observed time delay of these photons compared to photons that did not suffer any scattering can be calculated in two alternative ways: (a) calculation of the diffusion time delay in an expanding plasma, as was done here; and (b) since these photons are advected outward with the flow from the emission radius  $r_D$  to the photospheric radius,  $r_{ph}$ , the time delay should be equal to the ‘‘geometrical’’ time delay of photons emerging from  $r_{ph}$ . Here, we show that the two different approaches lead to the same result, provided the optical depth at the dissipation radius is high and that the plasma expands at velocity close to  $c$ .

In order to include a variety of possible dissipation mechanisms (such as, e.g., magnetic reconnection), we assume that the comoving width of the plasma at the dissipation radius is arbitrary, and denoted by  $\Delta r_D$ . At larger radii  $r > r_D$  the dissipated region is advected with the flow, therefore the width of this region increases with radius,  $\Delta r \propto r$ . For a single (not continuous) energy release, the number density of protons at radius  $r$  is  $n_p(r) = E/(4\pi r^3 m_p c^2)$ , thus the optical depth at radius  $r$  is

$$\tau(r) = \frac{E\sigma_T\Delta r_D}{4\pi r_D r^2 m_p c^2} \quad (B1)$$

where  $\Delta r(r) = \Delta r_D(r/r_D)$ . The photospheric radius is given by  $r_{ph} = r(\tau = 1)$ , or

$$r_{ph} = \left( \frac{E\sigma_T\Delta r_D}{4\pi r_D m_p c^2} \right)^{1/2}. \quad (\text{B2})$$

The diffusive time delay is approximated by

$$\Delta t_D^{ob.} \simeq \frac{\sqrt{\tau(r=r_D)\Delta r_D}}{\Gamma c} = \frac{r_{ph}}{\Gamma c} \frac{\Delta r_D}{r_D} = \frac{\Delta r(r_{ph})}{\Gamma c}. \quad (\text{B3})$$

We thus find that the diffusive time delay is similar to the time delay resulting from the finite width of the plasma at the photospheric radius (see Waxman 1997). In addition, photons that are emitted at the photospheric radius from a point not on the line of sight suffer a time delay  $\sim r_{ph}/\Gamma^2 c$ , which is thus the minimum observed time delay. For the specific case of dissipation by internal shock waves, the comoving width is  $\Delta r = r/\Gamma$ , the time delay due to the finite width of the plasma is similar to the time delay due to emission from positions off the line of sight, and we obtain the familiar result  $\Delta t_D^{ob.} \simeq r_{ph}/\Gamma^2 c$ . However, the above analysis shows that in the more general case of arbitrary plasma width  $\Delta r > r/\Gamma$ , the diffusive time delay is equal to the time delay due to the finite width of the plasma, which determines the observed time delay.

#### REFERENCES

- Aloy, M. A., Müller, E., Ibañez, J., Martí, J., & MacFadyen, A. 2000, *ApJ*, 531, L119  
 Barthelmy, S.D., *et al.* 2005, *Space Science Reviews*, 120, 143  
 Barthelmy, S.D., *et al.* 2005, *ApJ*, 635, L133  
 Burrows, D.N., *et al.* 2005, *Space Science Reviews*, 120, 165  
 Chincarini, G., *et al.* 2005, *ApJ*, submitted (astro-ph/0506453)  
 Cusumano, G., *et al.* 2006, *ApJ*, 639, 316  
 Dermer, C. 2004, *ApJ*, 614, 284  
 Fenimore, E.E., Madras, C.D., & Nayakshin, S. 1996, *ApJ*, 473, 998  
 Gehrels, N., *et al.* 2004, *ApJ*, 611, 1005  
 Giannios, D., & Spruit, H. 2005, *A&A*, 430, 1  
 Hill, J.E., *et al.* 2006, *ApJ*, 639, 303  
 Kouveliotou, C., *et al.* 1993, *ApJ*, 413, L101  
 Kumar, P., & Panaitescu, A. 2000, *ApJ*, 541, L51  
 Lazzati, D., & Begelman, M.C. 2005, *ApJ*, 629, 903  
 Levinson, A., & Eichler, D. 1993, *ApJ*, 418, 386  
 Liang, E.W., *et al.* 2006, *ApJ*, in press (astro-ph/0602142)  
 MacFadyen, A.I., & Woosley, S.E. 1999, *ApJ*, 524, 262  
 MacFadyen, A.I., Woosley, S.E., & Heger, A. 2001, *ApJ*, 550, 410  
 Matzner, C.D. 2003, *MNRAS*, 345, 575  
 Matzner, C.D., & McKee, C.F. 1999, *ApJ*, 510, 379  
 Mészáros, P., & Rees, M.J. 2001, *ApJ*, 556, L37  
 Nousek, J.A., *et al.* 2005, *ApJ*, 642, 389  
 O'brien, P.T., *et al.* 2006, *ApJ*, in press (astro-ph/0601125)  
 Paczyński, B. 1998, *ApJ*, 494, L45  
 Pe'er, A., & Waxman, E. 2004, *ApJ*, 613, 448  
 Pe'er, A., Mészáros, P., & Rees, M.J. 2005, *ApJ*, 642, 995  
 Pe'er, A., & Wijers, R.A.M.J. 2005, *ApJ*, in press (astro-ph/0511508)  
 Ramirez-Ruiz, E., Celotti, A., & Rees, M.J. 2002, *MNRAS*, 337, 1349  
 Rybicki, G.B., & Lightman, A. P. 1979, *Radiative Processes in Astrophysics* (New York: Wiley)  
 Sunyaev, R.A., & Titarchuk, L.G. 1980, *Astron. Astrophys.* 86, 121  
 Tagliaferri, G., *et al.* 2005, *Nature*, 436, 985  
 Thompson, C. 1994, *MNRAS*, 270, 480  
 Vaughan, S., *et al.* 2006, *ApJ*, 638, 920  
 Waxman, E. 1997, *ApJ*, 491, L19  
 Waxman, E., & Mészáros, P. 2003, *ApJ*, 584, 390  
 Woosley, S.E. 1993, *ApJ*, 405, 273  
 Woosley, S.E. 1999, in *AIP Conf. Proc.* 526, Fifth Huntsville Symp. on Gamma-Ray Bursts, ed. R.M. Kippen, R.S. Malozzi, & G.J. Fishman (New York: AIP), 555  
 Zhang, B., *et al.* 2006, *ApJ*, 642, 354  
 Zhang, W., Woosley, S.E., & MacFadyen, A.I. 2003, *ApJ*, 586, 356